



## Estimation of tool wear during CNC milling using neural network-based sensor fusion

N. Ghosh<sup>a,\*</sup>, Y.B. Ravi<sup>b</sup>, A. Patra<sup>c</sup>, S. Mukhopadhyay<sup>c</sup>, S. Paul<sup>d</sup>,  
A.R. Mohanty<sup>d</sup>, A.B. Chattopadhyay<sup>d</sup>

<sup>a</sup>Department of Electrical Engineering, University of California, Riverside, CA 92521-0425, USA

<sup>b</sup>GE Research, John F. Welch Technology Center, Bangalore 560066, India

<sup>c</sup>Department of Electrical Engineering, Indian Institute of Technology, Kharagpur, West Bengal 721302, India

<sup>d</sup>Department of Mechanical Engineering, Indian Institute of Technology, Kharagpur, West Bengal 721302, India

Received 20 October 2004; received in revised form 21 July 2005; accepted 19 October 2005

Available online 3 February 2006

---

### Abstract

Cutting tool wear degrades the product quality in manufacturing processes. Monitoring tool wear value online is therefore needed to prevent degradation in machining quality. Unfortunately there is no direct way of measuring the tool wear online. Therefore one has to adopt an indirect method wherein the tool wear is estimated from several sensors measuring related process variables. In this work, a neural network-based sensor fusion model has been developed for tool condition monitoring (TCM). Features extracted from a number of machining zone signals, namely cutting forces, spindle vibration, spindle current, and sound pressure level have been fused to estimate the *average flank wear of the main cutting edge*. Novel strategies such as, signal level segmentation for temporal registration, feature space filtering, outlier removal, and estimation space filtering have been proposed. The proposed approach has been validated by both laboratory and industrial implementations.

© 2005 Elsevier Ltd. All rights reserved.

**Keywords:** Data fusion; Back propagation neural network; Tool condition monitoring; Signal segmentation; Feature space filtering; Outliers

---

### 1. Introduction

In a Machining Center, due to thermal fracturing, attrition, abrasion, plastic deformation, diffusion, chemical wear, and grain-pullout, the cutting tool gradually wears out, loses its sharpness and becomes blunt (Fig. 1). This affects the machining process and the health of the machine tool as well. Blunt tools lead to unwanted vibration, which spoils the surface finish and causes dimensional inaccuracy. In the worst case, the cutting tool may break while it is engaged with the work-piece. Sudden release of the load and consequential

---

\*Corresponding author. Tel.: +1 951 544 3663; fax: +1 951 787 2425.

E-mail addresses: nirmalya@ee.ucr.edu (N. Ghosh), ravi.yb@ge.com (Y.B. Ravi), amit@ee.iitkgp.ernet.in (A. Patra), smukh@ee.iitkgp.ernet.in (S. Mukhopadhyay), spaul@mech.iitkgp.ernet.in (S. Paul), amohanty@mech.iitkgp.ernet.in (A.R. Mohanty), abcme@mech.iitkgp.ernet.in (A.B. Chattopadhyay).

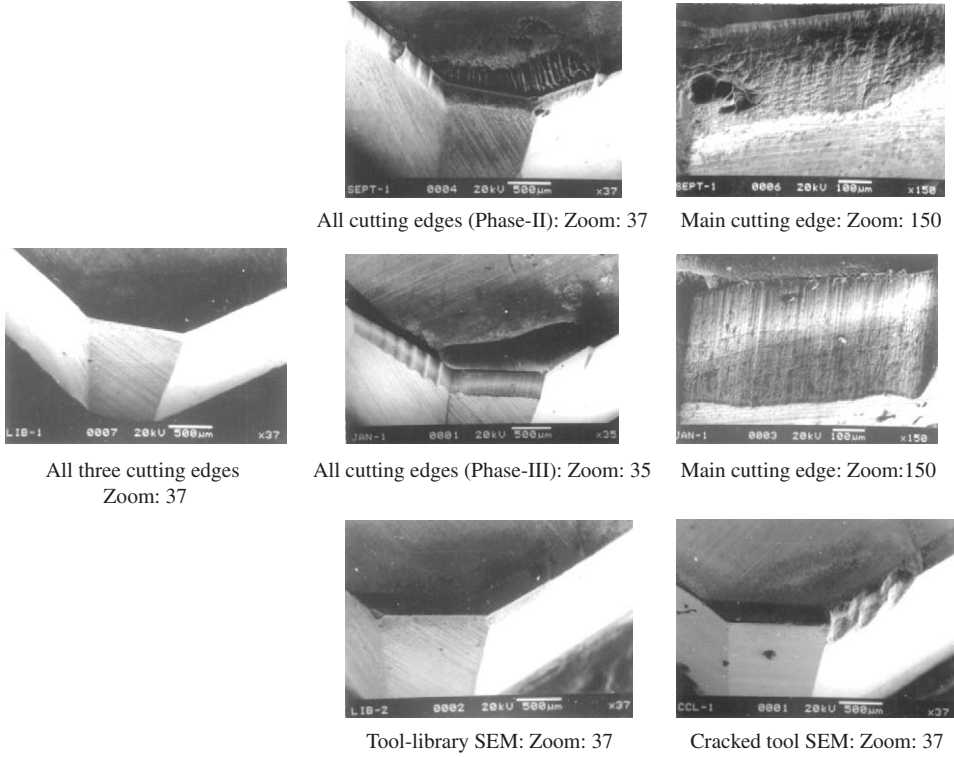


Fig. 1. Representative scanning electron microscopy (SEM) figures of tool wear.

inertial effects can leave incurable stress effects on the costly work-piece as well as the machining center. Estimation of the tool wear can help decide about possible optimization of the machining parameters (cutting speed, feed, and depth of cut) or replacing the worn out tool with a fresh tool. Estimation of tool wear can be done by several offline methods, like volumetric measurements, and microscopic measurements. Although these offline processes are quite accurate, they are not cost effective for the industries as they consume valuable machining time and hence reduce productivity. Hence manufacturing industries need an online system that continuously monitors the tool wear condition while the machining continues.

In the recent years, a few researchers have worked on the application of laser- and video-based online artificial vision systems for direct online tool condition monitoring (TCM) [20,21,29]. But high cost and inconsistency due to variation in illumination have prevented this method from being implemented in the industry. A more economic proposition is to use an indirect method of monitoring tool wear from measured signals (which are affected by tool condition) like cutting force [4,5,8,10,11,12], machine vibration [8], motor load current [26], acoustic emission (AE) from the machining zone [16,17,25] or various combinations of these signals [8]. In application specific domains, this indirect method of monitoring works reasonably well. But unfortunately, most of the indirect online TCM systems developed so far are tested on the turning process [1,14,15,26,28]. Turning is a fixed-tool machining process that generates continuous signals. Therefore these systems are not guaranteed to work satisfactorily for a semi-intermittent process like grinding or a fully intermittent process like milling. Recent attempts in developing TCM for drilling [13], end milling [9,24], and face milling [11,12] lack the data fusion strategies in the true sense proposed in some innovative works [3,6,23], because a particular signal may not work well for a particular machining process. As for example, use of AE has been reported as not being that helpful for processes like milling or grinding [17,18]. Machining centers usually have automatic tool changers (ATC) and utilise most of the different machining processes to carve out complex products. So a practical online TCM system requires to function well for different machining processes for industrial acceptability. Most of the present-day TCM systems lack this capability and hence a commercial scale TCM is yet to appear in the market.

So it is considered worthwhile to investigate the nature of the signals and their dependency on tool wear, specifically for an intermittent machining process, like face milling. Some of the recent works [11,12] have used cutting force signal and Artificial Neural Network (ANN) in TCM for face milling process. But cutting force based TCM is a costly proposition due to sensor cost and mounting problems. The aim of this work is to design a low-cost solution acceptable to the industry. The main features of this work are:

- *Use of multiple sensors:* Different signals are correlated differently to the tool condition at different levels of tool wear. As no clear idea has emerged regarding which signal is effective at what level of tool wear in the entire tool life, an adaptive (or intelligent) fusion of the number of signals is proposed in this work. Sensor signals have been used individually and in various combinations by adaptive sensor fusion method to predict the average flank (main cutting edge) wear level of the cutting tool.
- *Signal level segmentation:* As mentioned above, the main difference between the turning process and the face milling process (the case in hand) is the lack of continuity of the latter. Although multiple insert face milling is more natural in industrial conditions, it increases complexity due to multiple insert engagement at the same time and hence signals for all engaged inserts are added producing intractability. As the focus of this work is feasibility of online TCM implementation, single insert face milling simplification has been undertaken. Due to intermittency of the face milling process, tool condition information is available only in the machining time segments of the signals. Hence signal level segmentation has been implemented.
- *Sensor fusion through ANN:* It is known that fusion of multiple signals that are correlated with the same process parameter can estimate that parameter better. This is because different signals have different correlation efficiency and their effective and cooperative fusion is expected to produce better estimation result. In this work, ANN has been used as the tool for feature level Sensor Fusion (SF) with offline training and online prediction capability.
- *Feature space filtering:* Note that the time-samples of the signals acquired from the process have much higher frequency content than the quantity of interest, the tool wear variation over the machining period. For obvious reasons tool wear variation is a monotonically increasing function. But unavoidable variations in features due to mechanical noises make fluctuating estimations. Hence signal features are filtered at different levels of estimation process.
- *Experiments conducted both in laboratory and industrial environment:* Differences in noise levels and environmental conditions exist between laboratory and industrial environments. In this work, training data, collected from tool-life experiments conducted both in the laboratory and industrial face milling centers have been used for model building.

The rest of the paper is organised as follows. Section 2 briefly describes the system architecture and hardware/software used to implement the same. Signal processing techniques and sensor fusion strategies adopted in this work are discussed in Section 3. Results for various models are presented in Section 4 showing improvements with sensor fusion. Section 5 concludes the paper summarizing the contribution of this work and future scope.

## 2. System architecture

The architecture of the whole system is shown in Fig. 2. To estimate cutting tool wear from real-time signals tapped from machining environment, signals that are most sensitive to tool condition need to be considered. On the basis of the literature survey on TCM and prior experiences in similar research, the following process signals have been selected.

- three-axes dynamometer for cutting force signals;
- Hall effect current probe for spindle motor current;
- Hall effect voltage sensor for spindle motor supply voltage;
- 1-axis accelerometer for spindle vibration signal;
- three-axes accelerometer for work-piece vibration signals;

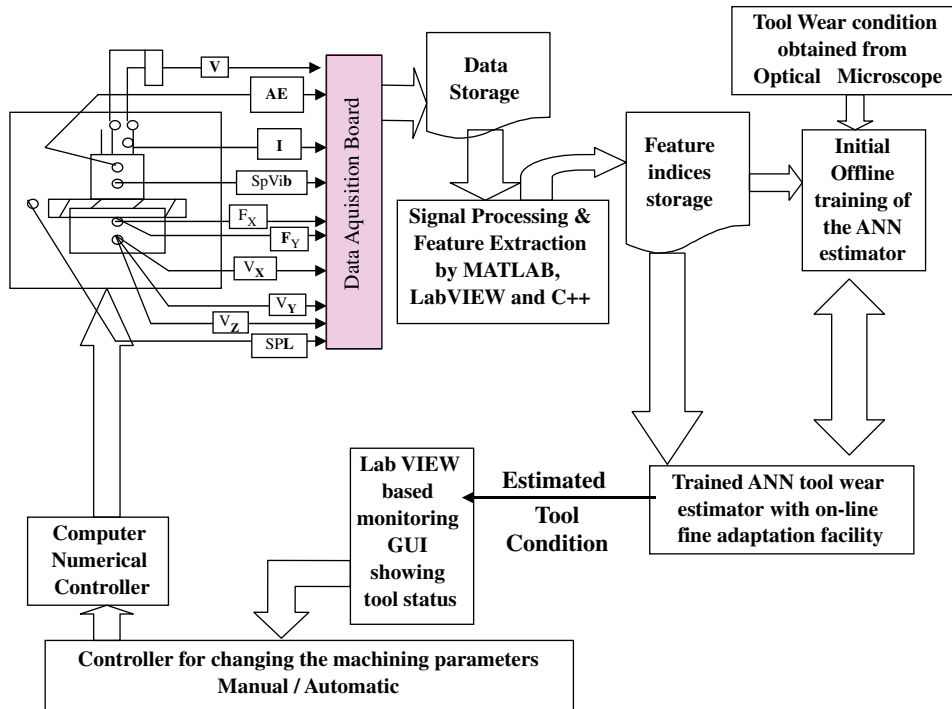


Fig. 2. System architecture.

- microphone for machining sound signal;
- AE sensor.

Signals from these sensors are acquired in a PC through two data acquisition cards. The raw signals undergo several steps of digital signal processing, appropriate to reduce noise, segment the machining time signals and extract features. The average tool wear of the main cutting edge is manually measured by an optical microscope and, together with the feature vector, forms the training set of the ANN. The feedforward ANN module is trained by the standard back-error-propagation learning rule.

After the ANN-decision system is trained offline, that is during the online estimation phase, signal features are fed to the trained ANN and tool wear estimation is obtained in real time.

### 3. Signal processing and sensor fusion

Signals acquired from a machining center in an industrial environment contain high levels of mechanical, electrical and acoustic noises. Also, as mentioned earlier, in intermittent face milling process, signals carry useful information on cutting tool condition only when the cutting tool is in contact with the work-piece. Hence appropriate signal processing is mandatory before extracting features. The technique followed is detailed in the following subsections.

#### 3.1. Segmentation

Signal-level temporal segmentation is needed to extract the signal lobes during the time the tool is actually removing metal, since only these lobes contain information about tool wear condition. The first step in segmentation is the removal of incomplete lobes which may exist at either ends of a given raw signal sequence. This is then processed with low-pass filter to remove the high frequency noise from the measurements. In the next step the machining lobes are extracted by identifying the time points corresponding to engagement and

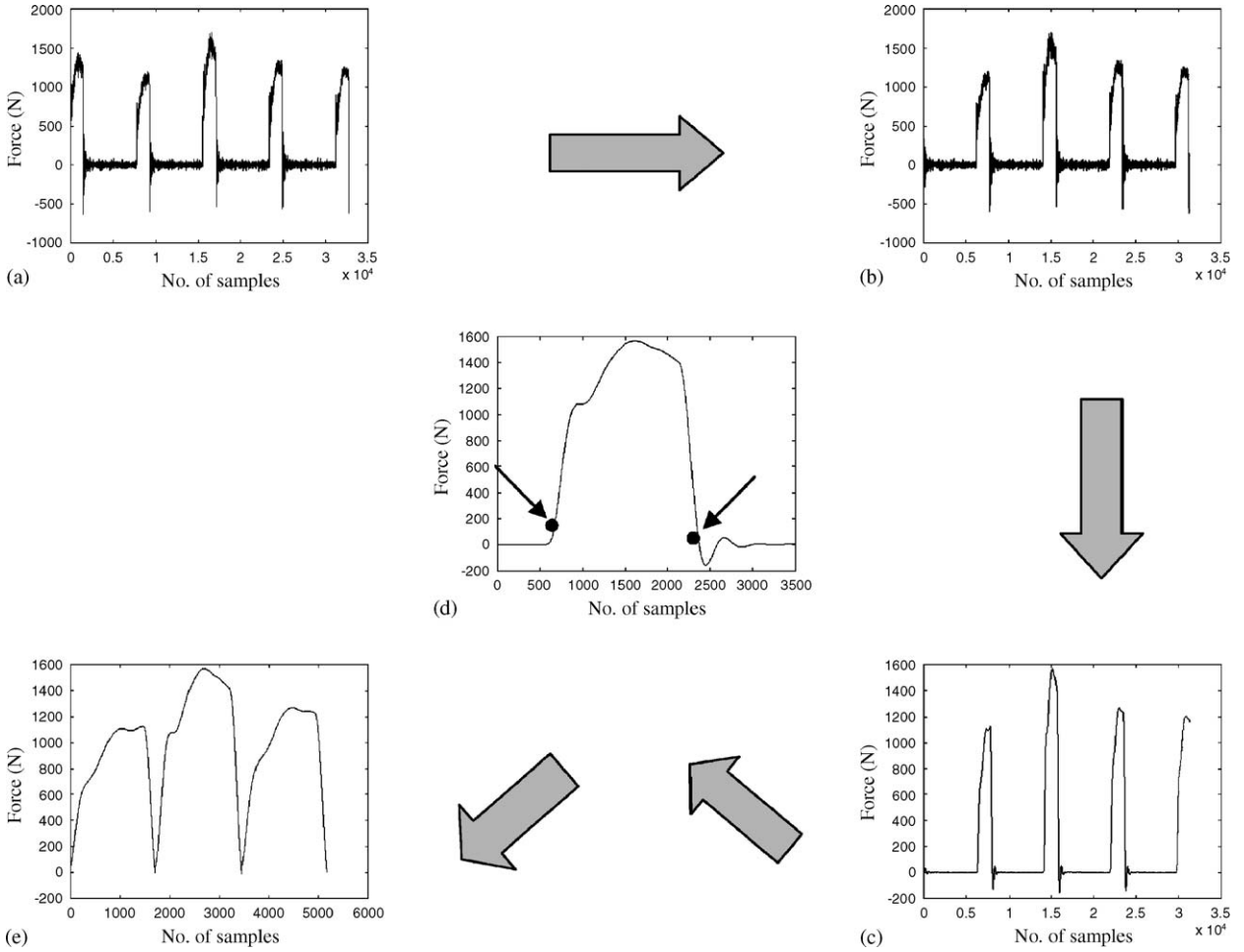


Fig. 3. Signal processing modules: (a) raw signal; (b) chopped signal; (c) filtered signal; (d) entry and exit points; and (e) segmented signal.

disengagement of the cutting tool and work-piece. Statistical change detection techniques are applied to make this step robust against noisy peaks. Fig. 3 gives a schematic diagram of the segmentation steps. Brief details of each of these steps are given below.

### 3.1.1. Elimination of incomplete lobes

Chopping is to be carried out before the low-pass filtering because, the latter step gives rise to a time delay that would give rise to a problem in distinguishing between machining and non-machining periods. Further the lobes would tend to get flattened and useful information during the machining period would be lost. Hence, from the initial few sampling points in the signal sequence, it is statistically decided whether the sequence starts with a machining phase or a non-machining one. For signals starting with a machining phase, initial incomplete lobe is deleted for correct average features to be computed in the later stage. Incomplete lobes at the end of the captured signals are also deleted similarly.

### 3.1.2. Temporal registration between signals

Due to unavoidable (and sometime variable as well) inbuilt time delays of different sensors and the signal acquisition circuitry, it is not guaranteed that  $T$ th sampled values of different signals carry the same machining information at time-instant  $T$ . This is generally ensured by formal programmatic temporal registration. For feature level sensor fusion (see Section 3.3), it is mandatory to have different signals to be temporally registered, so that the features of different signals at the same time instant carry a true signature of the mapped

output state at that particular time. Hence machining lobes extracted from different signals should be temporally registered. This requires a marker signal, indicating the entry and exit points of the machining time lobes for itself and all other signals. This reduces the computational complexity of finding machining lobes separately for each signal, since, for signals like electrical supply voltage, load current to the spindle motor, and sound pressure level (SPL), it is difficult to define these lobes independently.

Experimentally, longitudinal cutting force signal ( $F_X$ ) has been found to be the best candidate as the marker signal. Incomplete lobes are marked from  $F_X$  signal, and corresponding temporal regions of all the signals are deleted.

### 3.1.3. Low-pass filtering of segmented signals

Since the machining frequency has been between 4.16 and 9 Hz corresponding to, cutting velocity 98–212 m/min, cutter diameter 125 mm and single insert case, force signals ( $F_X$  and  $F_Y$ ) are expected to contain tool condition information only in frequency components below 10 Hz. Current ( $I$ ) and voltage ( $V$ ) signals are expected to be within the same frequency range although modulated by the supply frequency (50 Hz). Significant frequency bands for signals such as the work-piece-vibration, spindle-vibration, AE and SPL signals have been decided similarly considering the sensor-specifications and environmental effects (like human speech signals affecting SPL signal). Fourth-order Butterworth low-pass filters are designed and implemented for filtering the acquired signals after segmentation.

### 3.1.4. Statistical state transition and segmentation

Even after filtering, small noise peaks are still present in the signals close to machining signal frequency. In the presence of these, transitions between machining state (high cutting force) and non-machining state (nominal force) are detected statistically to avoid spurious lobes. A change in signal level is compared with a threshold periodically for certain times and a transition is detected only if the change exceeds the threshold for all the checks.

In this way, all the machining lobes in the marker  $F_X$  signal are marked. And then using these marked transition time points, all the other signals are segmented (see temporal registration) into machining and non-machining parts. Only the machining segments of each signal are considered for feature extraction.

## 3.2. Feature space filtering

In this work, to start with, only the simplest features have been selected to ensure feasibility of real-time implementation. Features (e.g. maxima, minima, peak-to-peak, mean, standard deviation, root-mean-square (RMS) values, and normalised ratios) have been computed for each lobe and then averaged over segmented complete lobes. The feature vectors are composed of a set of these features according to their efficacy in predicting the wear value. Average RMS features of  $F_X$ ,  $F_Y$ ,  $I$ , and  $V$  signals and instantaneous spindle motor input power  $P$  (calculated from values of  $I$  and  $V$  by point-to-point multiplication) have been found to be the most informative. Few of the used feature trends are shown in Fig. 4.

Although tool-wear is a gradually monotonically increasing process, due to high frequency noises, oscillations are seen in the feature trends of Fig. 4. These are due to transient mechanical events, like breaking of a built-up-edge (BUE), local hardness variation over the work-piece, fluctuation in supply voltage and similar factors. It is clear that the features computed above are not suitable for direct usage in estimation of the tool wear.

So to improve the overall estimation of the monotonically increasing tool wear curve, the high frequency fluctuations in feature space are filtered out before training the neuro-estimator.

A third-order Butterworth low-pass filter given below has been used to reduce the fluctuations.

$$\frac{X_{\text{filtered}}}{X} = \frac{10^{-4} * (0.0376 + 0.1127z^{-1} + 0.1127z^{-2} + 0.0376z^{-3})}{1 - 2.9372z^{-1} + 2.8763z^{-2} - 0.9391z^{-3}}.$$

To avoid errors for zero initial conditions, three initial samples of feature values are used as initial conditions of the filter. The output of feature space filtering for the force signals  $F_X$  and  $F_Y$  are shown in Fig. 5. Using these filtered features for training the ANN neuro-estimator (see Section 3.3), the training level of the estimator could be improved by a marked degree.

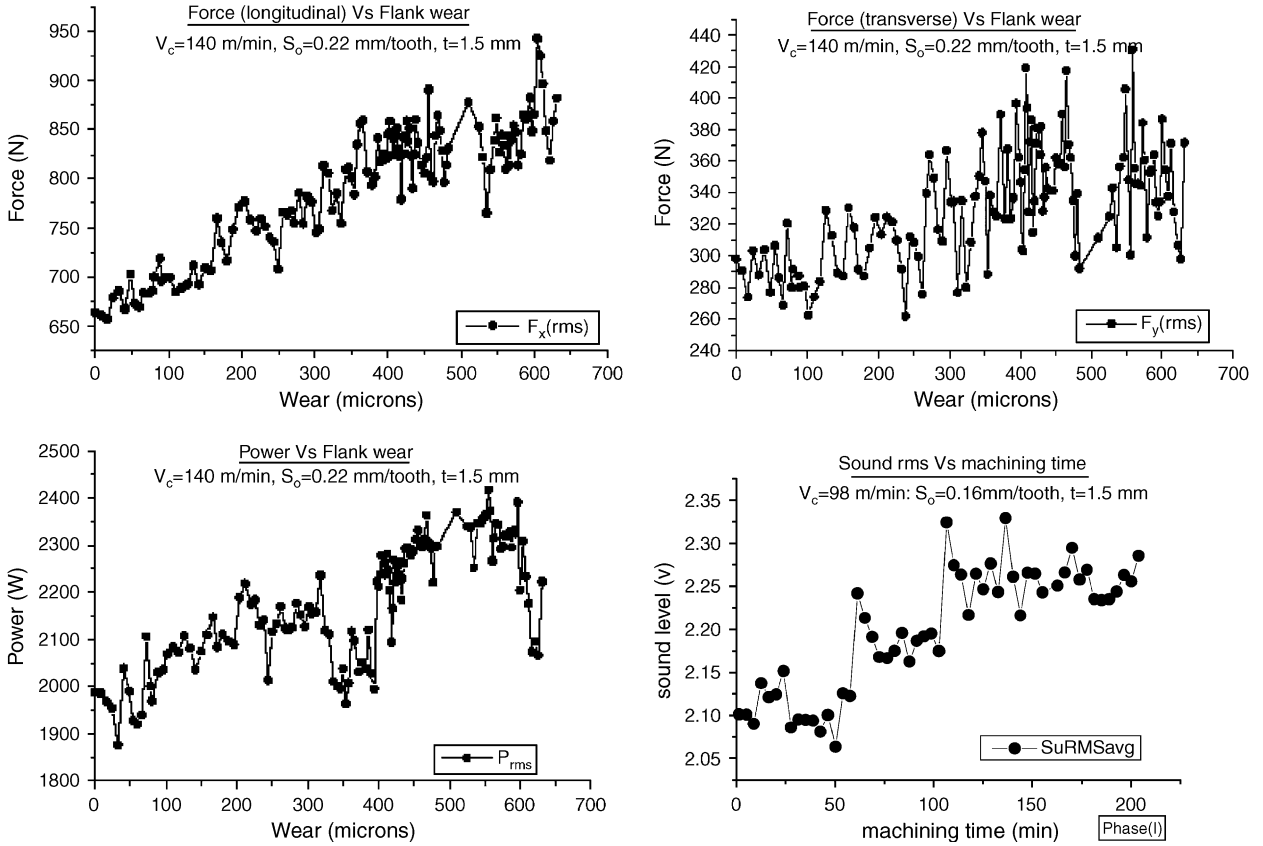


Fig. 4. Example RMS feature trends with tool-wear.

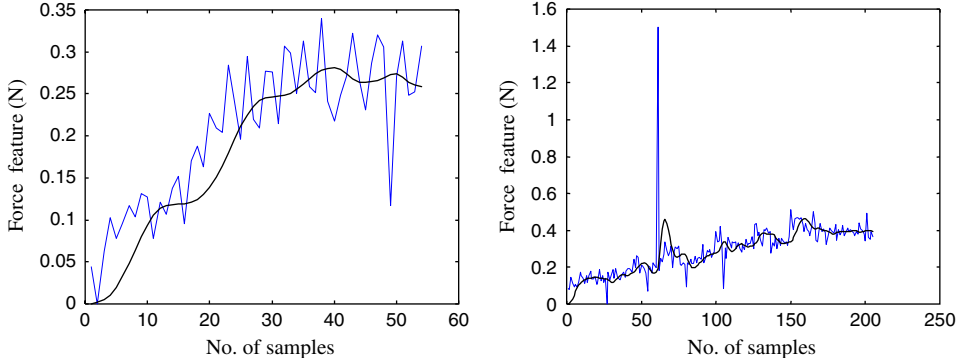


Fig. 5. Effect of feature space filtering. Left:  $F_y$  RMS feature; Right:  $F_x$  RMS feature.

After features are saved as datasets, each of the data vector, including the actual tool-wear value as observed under an optical microscope, has been used as one exemplar for the supervised training of the estimator.

### 3.3. Sensor fusion using ANN

It is well known from recent research that an estimator that employs multiple sensors using sensor fusion techniques provides improved and robust estimates. In this work, therefore an estimator has been designed that employs a feature level fusion of signals obtained from different sensors.

Among different tools to fuse the signal features, like mathematical functions, distributed blackboard architecture [9], rule-based fuzzy sets, genetic algorithms, and ANN [2], in this work ANN has been selected. This is because, dependence of different signals with tool wear is too complex to be expressed in mathematical form [27] and no expert Boolean rule-based knowledge base can be developed with enough generality and fidelity. An ANN provides the advantage of non-linear mapping of signal features to tool wear that can be learnt from the training data when explicit mathematical mapping model behind it is of less importance and hence may be considered as a black-box [2,19]. Note that ANNs have been used in TCM earlier as well [3,4,6,7,10–12,15,27], though mostly for the turning process and with a limited number of machining signals.

Sensor fusion induces advantages-like redundancy, complementariness, and less costly implementation, while ANN instills complex non-linear mapping, adaptability, and flexibility of the structure. The strategy developed here marries sensor fusion with feedforward ANN and is validated with satisfactory results in a real-time error-prone environment. In this work, among a plethora of training rules, the well-known back-error-propagation learning rule has been adopted with gradient descent principle in batch mode for robustness (to occasional misleading individual exemplars). To ensure generality of the back propagation neural network (BPNN) few measures have been taken in this work as follows:

- *Datasets representing whole feature space:* To ensure this, three (training, testing and validation) datasets have been generated completely randomly and independently satisfying mutual exclusiveness and the same mean and standard deviation within individual datasets.
- *Over-fitting prevention for generality:* This is ensured by periodically checking with testing dataset in between training set-based learning iterations. If both the training error and the test error continue to drop (measured statistically to avoid some of the local minima), then only learning process is continued.

An important criterion of success of any ANN-based sensor fusion strategy is the proper selection of feature sets used as mapping input [22]. In this work, cross-correlation chart (in Table 1) is computed and then different collections of features from highly correlated signals have been used for fusion.

A fully connected BPNN with two hidden layers (X-10-5-1, where X depends on size of input feature vector), a log-sigmoid activation function with unity slope, 0.9 learning rate and 0.9 momentum parameters has been used. The above configuration has been found successful after considerable fine-tuning. The high learning rate and momentum parameters are motivated from the need to have a fast learning in the face of feature variations present, and with relatively less number of training exemplars for the complex and dynamic non-linear mapping model. High learning rate leads to fast learning, and high momentum term (due to differential control nature [22]) guarantees that the error reduction curve is reasonably smooth.

The sensor fusion-based ANN estimator has been implemented in C++ using Microsoft Visual C++ editor and compiler. A typical ANN sensor fusion structure is shown schematically in Fig. 6.

Table 1  
Cross-correlation chart (with avg. coefficients) for raw signals

	$F_X$	$F_Y$	$V_{\text{Spindle}}$	$V_X$	$V_Y$	$V_Z$	$SPL$	$I_{\text{Spindle}}$	$Vol_{\text{Spindle}}$	$P_{\text{Spindle}}$
$F_X$	1	0.868	0.001	0.05	0.084	0.03	0.43	0.076	0.054	0.616
$F_Y$	0.868	1	0.001	0.01	0.166	0.045	0.35	0.082	0.055	0.569
$V_{\text{Spindle}}$	0.001	0.001	1	0.321	0.396	0.42	0	0.03	—	—
$V_X$	0.05	0.01	0.321	1	0.130	0.22	0	0.05	—	—
$V_Y$	0.084	0.166	0.396	0.130	1	0.45	0.12	0.03	—	—
$V_Z$	0.03	0.045	0.42	0.22	0.45	1	0	0.01	—	—
$SPL$	0.43	0.35	0	0	0.12	0	1	0.1	—	—
$I_{\text{Spindle}}$	0.076	0.082	0.03	0.05	0.03	0.01	0.1	1	0.882	0.023
$Vol_{\text{Spindle}}$	0.054	0.055	—	—	—	—	—	0.882	1	0.041
$P_{\text{Spindle}}$	0.717	0.569	—	—	—	—	—	0.023	0.041	1

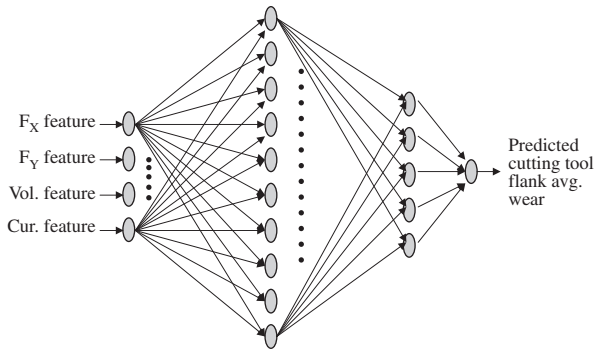


Fig. 6. One typical sensor fusion-based neuro-estimator structure.

### 3.4. Prediction space filtering

Due to unpredictable and unavoidable nature of disturbances present in the source environment, and due to inherent local minima problem in ANNs, even after considerable number of training iterations, predicted tool wear shows some oscillations. But average tool wear value increases monotonically, and hence predicted wear curve is also expected to be a monotonically non-decreasing one. To ensure this, two measures have been adopted:

1. Some extreme cases of outliers (like one shown in right graph of Fig. 5) are eliminated, since the effects of these are difficult to be removed by feature space filtering.
2. The output tool wear trend is filtered with third-order Butterworth IIR filter. This has improved results by reducing the error to almost half of its previous value.

## 4. Results and discussion

Several machining experiments have been conducted in three face-milling machining centers: (1) one Batliboi conventional face-milling machine and (2) one LMW CNC machining center in the lab environment and (3) one CNC Plano-Miller *in industrial environment* (*at Flanders Ltd, Kharagpur, India*) using the same face-milling cutter (125 mm diameter), single uncoated tungsten-carbide (WIDIA-SPKN 1203EDR TTMS) cutting tools over wide variations of machining parameters (cutting velocity: 98–212 m/min, cutting feed: 0.08–0.22 mm/tooth, depth of cut: 1.5–2 mm). Different types of experiments have been conducted, like tool-library experiments (for initial feature selection), extended tool-life experiments (for ANN training) and again tool library experiments and cracked tool experiments (for ANN validation, see Fig. 1) on C-60 steel work-pieces. Sensor fusion strategies have evolved gradually by taking into account performance of different signals in previous experiments. Actually five datasets (Datasets: I–V; *last two in industrial environment*) have been tried in this work. Only candidate prediction results are shown in this paper due to space constraints.

### 4.1. Cross-correlation chart

As discussed in the last section, to decide on the combination of signals that should be used for sensor fusion, a cross-correlation measure has been adopted. The result is shown in Table 1. In some cases cross-correlations could not be found because the signals were curtailed from acquisition list due to poor performance in previous phase and new sensors being considered in their places.

As can be seen, cutting force signals are well correlated (as expected) while spindle motor current and voltage signals are also well correlated (this is also expected). SPL also shows a fair correlation with cutting force signals.

But most significant is the correlation of electrical input power signal  $P$  (to the spindle motor) and the cutting force signal as seen in Fig. 7. This result has prompted us to propose a cost effective online TCM solution based on power instead of the force-based counterpart using costly dynamometers.

#### 4.2. Prediction results of sensor fusion

##### 4.2.1. Using cutting force features

Initially cutting force features have been used to predict tool wear for benchmarking. The sensor fusion results are shown in Figs. 8 and 9 with and without feature space filtering, respectively. They also illustrate the need for feature space filtering.

The results are comparable to other recent works in TCM [1]. Using cutting parameters as input to the neuro-predictor, the strategy has been verified for all datasets, as shown in Fig. 10. The ANN could learn even

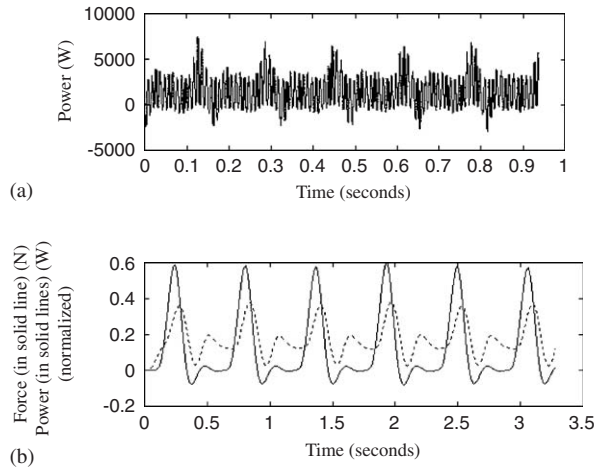


Fig. 7. (a) Spindle input power-index ( $P$ ) signal and (b) filtered  $F_x$  and filtered power signal superimposed for comparison.

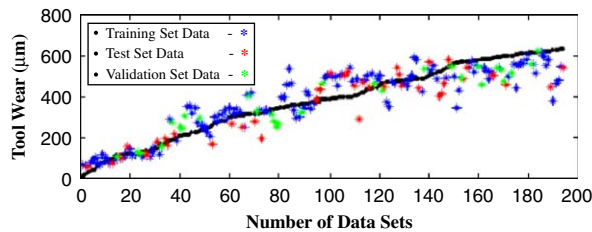


Fig. 8. Estimation with unfiltered force (RMS) features of dataset-III: feature specification: unfiltered; structure: 2-10-5-1; maximum iteration: 1,000,000; learning rate: 0.9; momentum parameter: 0.9; avg. training error: 72  $\mu\text{m}$  and avg. test error: 75  $\mu\text{m}$ .

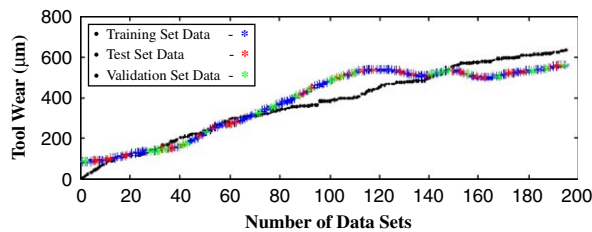


Fig. 9. Estimation with filtered force (RMS) features of dataset-III: feature specification: filtered; structure: 2-10-5-1; maximum iteration: 1,000,000; learning rate: 0.9; momentum parameter: 0.9; avg. training error: 57  $\mu\text{m}$  and avg. test error: 57  $\mu\text{m}$ .

few critical parameter changes during *Dataset-V (in industry)* when cutting parameters have been changed during the same tool-life experiment (note the kink in the zoomed version in Fig. 10) due to industrial requirements.

#### 4.2.2. Using electrical power filtered features

When only electrical power signal (i.e. current and voltage signal) features have been used for tool wear estimation, the result was fair over the low and middle level of tool wear; but deteriorated in the higher range. The result is shown in Fig. 11.

#### 4.2.3. Using cutting force and electrical power features

Now to improve the mid-level wear prediction in force-based predictor and high-level wear prediction in power-based predictor, if both the sensors are fused, the prediction result improves in terms of a reduction of prediction error by nearly 20  $\mu\text{m}$ . As seen in the predicted wear curve in Fig. 12, both the above-mentioned ranges of wear are better predicted by the sensor fusion.

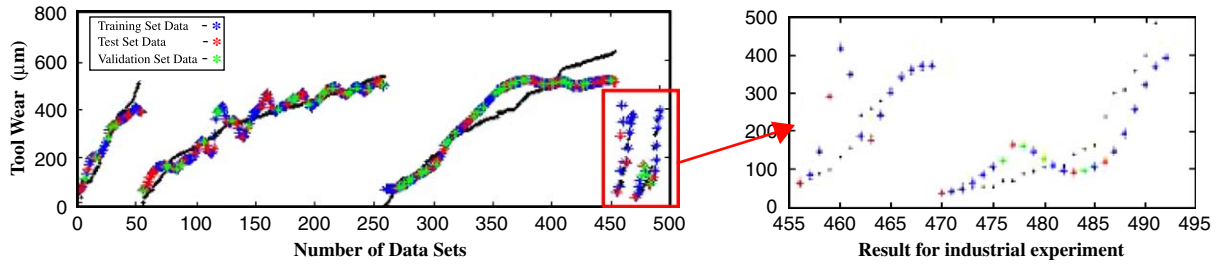


Fig. 10. Estimation with filtered force features from all five datasets: feature specification: filtered; structure: 5-10-5-1; maximum iteration: 1,000,000; learning rate: 0.9; momentum parameter: 0.9; avg. training error: 55  $\mu\text{m}$  and avg. test error: 59  $\mu\text{m}$ .

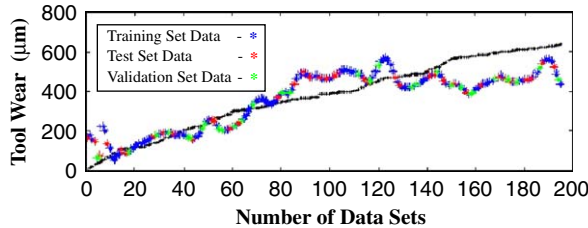


Fig. 11. Estimation with filtered current and voltage features of dataset-III: feature specification: filtered; structure: 2-10-5-1; maximum iteration: 1,000,000; learning rate: 0.9; momentum parameter: 0.9; avg. training error: 80  $\mu\text{m}$  and avg. test error: 80  $\mu\text{m}$ .

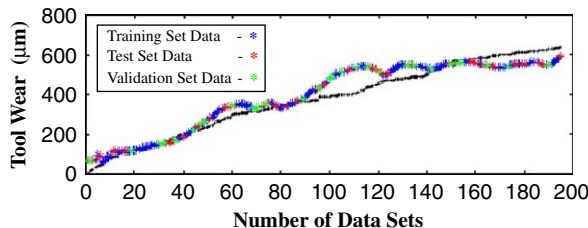


Fig. 12. Estimation based on forces, current and voltage (filtered) features: feature specification: filtered; structure: 4-10-5-1; maximum iteration: 5,000,000; learning rate: 0.9; momentum parameter: 0.9; avg. training error: 51  $\mu\text{m}$  and avg. test error: 47  $\mu\text{m}$ .

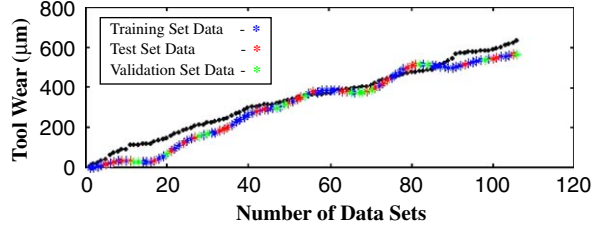


Fig. 13. Result with severe outliers rejection and estimation space filtering; dataset-III; feature specification: filtered; structure: 4-10-5-1; maximum iteration: 10,000,000; learning rate: 0.9; momentum parameter: 0.9; avg. training error: 23  $\mu\text{m}$  and avg. test error: 31  $\mu\text{m}$ .

Table 2  
Result summary (in training set average error levels in  $\mu\text{m}$ )

Different strategies	Dataset-I		Dataset-II		Dataset-III	
	UF	F	UF	F	UF	F
$F_X$ and $F_Y$	59	47	43	40	72	57
$I_{\text{Spindle}}$ and $Vol_{\text{Spindle}}$	—	—	—	—	73	80
$I_{\text{Spindle}}$ and $SPL$	55	49	52	50	—	—
$V_X$ , $V_Y$ and $V_Z$	128	120	123	115	—	—
$F_X$ , $F_Y$ , $V_X$ , $V_Y$ and $V_Z$	71	65	53	45	—	—
$F_X$ , $F_Y$ and $I_{\text{Spindle}}$	72	45	62	58	85	52
$F_X$ , $F_Y$ , $I_{\text{Spindle}}$ and $Vol_{\text{Spindle}}$	—	—	—	—	40	23
$F_X$ , $F_Y$ and $P_{\text{Spindle}}$	—	—	—	—	72	46
$F_X$ , $F_Y$ , $I_{\text{Spindle}}$ and $P_{\text{Spindle}}$	—	—	—	—	72	43

UF: no feature space filtering; F: feature space filtering.

#### 4.2.4. Using estimation space filtering

Due to the reasons mentioned in Section 3.4, if the two measures mentioned there are implemented in the sensor fusion strategy, then the prediction errors reduce to half of the last result with a much acceptable monotonic prediction curve as shown in Fig. 13, with force and power (filtered) features.

#### 4.3. Final result chart

Due to space constraint, a summary of results is tabulated in Table 2.

As mentioned, all results could not be computed due to unavailability of some signals in some of the datasets. From Table 2, RMS features of cutting force and spindle-motor input power outperformed all remaining sensor fusion schemes. Notably, spindle-motor current ( $I$ ) and  $SPL$  have also produced fairly good result and can be considered for an industrial implementation of TCM, as it is easier and cheaper to mount a microphone than a dynamometer. Best sensor fusion result has been obtained for the fusion of a dynamometer and Hall effect probes for sensing spindle motor electric voltage and current.

#### 5. Conclusion

From this work, following conclusions could be reached with a fair amount of confidence:

1. As expected, cutting force signal features predict tool wear fairly well.
2. Less costly and easily mountable current and voltage sensors can be a fairly good substitute of dynamometer (force sensor) for real industrial TCMs.

3. Techniques using multiple sensors improve TCM wear prediction over their single sensor counterparts. Like force and electrical power-based features outperform all the sensor-collections considered in this work.
4. Fusion of electrical current and SPL gives satisfactory prediction results.
5. As the integrated system (not detailed in this paper) is real time (predicts wear value within 0.85 s) and fairly accurate (prediction error below 25  $\mu\text{m}$ ), this approach has the potential of fulfilling industrial needs of online TCM.

It is to be noted that, though TCM based on estimated electrical input power to the spindle motor of the machine center performs fairly well, it is not the best of the lot (see Conclusion 3 and Table 2), as characterised by general sensor fusion for correlated signals. Hence depending on performance requirement and cost-effectiveness of critical machining processes, possibly low cost power-based TCM or SPL-current-based TCM can be used for general machining industry, while costly but better power and force-based TCM can be used for critical machining operations, like in machining of missile bodies.

### Acknowledgement

We sincerely thank Department of Information Technology (DIT), Government of India, for sponsoring the present project. We also take this opportunity to acknowledge M/S Flender (Ind.) Ltd., Kharagpur, India and M/s TATA Bearings Ltd., Kharagpur, India for providing excellent support and facilities during industrial trials and validation of the present work.

### References

- [1] M. Balazinski, E. Czogala, K. Jemielnaik, J. Leski, Tool condition monitoring using artificial intelligent methods, *Engineering Application of Artificial Intelligence* 15 (1) (2002) 73–80.
- [2] N.K. Bose, P. Liang, *Neural Network Fundamentals with Graphs, Algorithm, and Applications*, McGraw-Hill Publication, New York, 1995.
- [3] S.-L. Chen, Y.W. Jen, Data fusion neural network for tool condition monitoring in CNC milling machining, *International Journal of Machine Tools and Manufacture* 40 (2000) 381–400.
- [4] S. Das, R. Roy, A.B. Chattopadhyay, Evaluation of wear of turning carbide inserts using Neural Networks, *International Journal of Machine Tools and Manufacture* 36 (7) (1996) 789–797.
- [5] D.E. Dimla Sr., P.M. Lister, On-line metal cutting tool condition monitoring I: force and vibration analysis, *International Journal of Machine Tools and Manufacture* 40 (2000) 739–768.
- [6] D.E. Dimla Sr., P.M. Lister, Online metal cutting tool condition monitoring II: tool state classification using multi-layer perceptron neural networks, *International Journal of Machine Tools and Manufacture* 40 (2000) 769–781.
- [7] D.E. Dimla Jr., P.M. Lister, N.J. Leighton, Neural Network solutions to the TCM problem in metal cutting—a critical review of methods, *International Journal of Machine Tools and Manufacture* 37 (9) (1997) 1219–1241.
- [8] D.E. Dimla Sr., Sensor signals for tool wear monitoring in metal cutting operations—review of methods, *International Journal of Machine Tools and Manufacture* 40 (2000) 1073–1098.
- [9] R. Du, Signal understanding and tool condition monitoring, *Engineering Application of Artificial Intelligence* 12 (1999) 585–597.
- [10] R.K. Dutta, S. Paul, A.B. Chattopadhyay, Applicability of the modified back-propagation algorithm in tool condition monitoring for faster convergence, *Journal of Materials Processing Technology* 98 (2000) 299–309.
- [11] R.K. Dutta, G. Kiran, S. Paul, A.B. Chattopadhyay, Assessment of machining features for TCM in face milling using Artificial Neural Network, *Journal of Engineering Manufacture, Proceedings of the Institute of Mechanical Engineers Part B* 214 (B7) (2000) 535–546.
- [12] R.K. Dutta, S. Paul, A.B. Chattopadhyay, Fuzzy controlled back propagation neural network for tool condition monitoring in face milling, *International Journal of Production Research* 38 (13) (2000) 2989–3010.
- [13] T.I. El-wardany, D. Gao, M.A. Elbestaw, Tool condition monitoring in drilling using vibration signature analysis, *International Journal of Machine Tools and Manufacture* 36 (6) (1996) 687–711.
- [14] A. Ghasempoor, J. Jeswiet, T.N. Moore, Real-time implementation of on-line tool condition monitoring in turning, *International Journal of Machine Tools and Manufacture* 39 (1999) 1883–1902.
- [15] G.S. Hong, M. Rahman, Q. Zhou, Using Neural Network for Tool Condition monitoring based on Wavelet Decomposition, *International Journal of Machine Tools and Manufacturing* 36 (5) (1996) 551–556.
- [16] I. Inasaki, Application of acoustic emission sensor for monitoring machining processes, *Ultrasonics* 36 (1998) 273–281.
- [17] K. Jemielnaik, O. Otman, Tool failure detection based on analysis of acoustic emission signals, *Journal of Materials Processing Technology* 76 (1998) 192–197.
- [18] K. Jemielnaik, Some aspects of AE application in tool condition monitoring, *Ultrasonics* 38 (2000) 604–608.

- [19] S.V. Kamarthi, S. Pittner, Accelerating neural network training using weight extrapolations, *Neural Networks* 12 (9) (1999) 1285–1297.
- [20] S. Kurada, C. Bradley, A machine vision system for tool-wear measurement, *Tribology International* 30 (4) (1997) 295–304.
- [21] S. Kurada, C. Bradley, A review of machine vision sensors for tool condition monitoring, *Computers in Industry* 34 (1997) 55–72.
- [22] Y.-Z. Lu, *Industrial Intelligent Control: Fundamentals and Applications*, Wiley, New York, 1996.
- [23] R.C. Luo, M.G. Kay (Eds.), *Multisensor Integration and Fusion for Intelligent Machines and Systems*, Ablex Publishing Corporation, Norwood, NJ, 1995.
- [24] P.W. Prickett, C. Johns, An overview of approaches to end-milling tool monitoring, *International Journal of Machine Tools and Manufacturing* 39 (1999) 105–122.
- [25] H.V. Ravindra, Y.G. Srinivasa, R. Krishnamurthy, Acoustic emission for tool condition monitoring in metal cutting, *Wear* 212 (1997) 78–84.
- [26] T. Szecsi, A DC motor based cutting tool condition monitoring system, *Journal of Material Processing Technology* 92–93 (1999) 350–354.
- [27] T. Szecsi, Cutting force modeling using artificial neural networks, *Journal of Material Processing Technology* 92–93 (1999) 344–349.
- [28] T. Szecsi, Automatic cutting-tool condition monitoring on CNC lathes, *Journal of Materials Processing Technology* 77 (1998) 64–69.
- [29] Y.S. Wong, A.Y.C. Nee, X.Q. Li, C. Reisdorf, Tool condition monitoring using laser scatter pattern, *Journal of Materials Processing Technology* 63 (1997) 205–210.